AD-A166 277 EFFECT OF ENGINE DISCHARGING JET EFFLUX ON VEHICLE AERODYNAMIC PERFORMANCE(U) FOREIGN TECHNOLOGY DIV WRIGHT-PATTERSON AFB OH D YANG 24 FEB 86 1/1

UNCLASSIFIED FTD-ID(RS)T-1254-85 F/G 20/4 NL

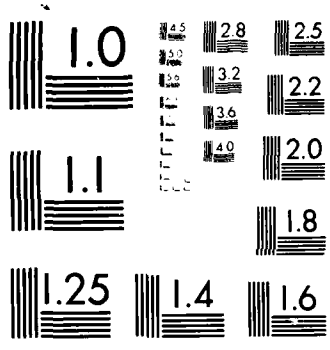

FTD-ID(RS)T-1254-85

FOREIGN TECHNOLOGY DIVISION

EFFECT OF ENGINE DISCHARGING JET EFFLUX ON VEHICLE AERODYNAMIC PERFORMANCE

by

Dao-wei Yang

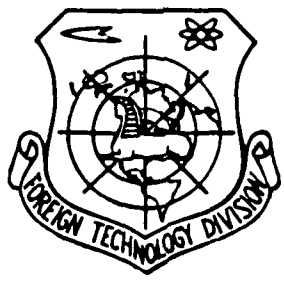

Approved for public release;
distribution unlimited.

EDITED TRANSLATION

FTD-ID(RS)T-1254-85 24 Feb 86

MICROFICHE NR: FTD-86-C-001531

EFFECT OF ENGINE DISCHARGING JET EFFLUX ON VEHICLE AERODYNAMIC PERFORMANCE

By: Dao-wei Yang

English pages: 9

Source: Binggong Xuebao (Beijing), No. 1, February 1985, pp. 45-50

Country of origin: China
Translated by: SCITRAN
F33657-84-D-0165
Requester: FTD/TQTA

PREPARED BY:

TRANSLATION DIVISION
FOREIGN TECHNOLOGY DIVISION
WP-AFB, OHIO.

GRAPHICS DISCLAIMER

All figures, graphics, tables, equations, etc. merged into this translation were extracted from the best quality copy available.

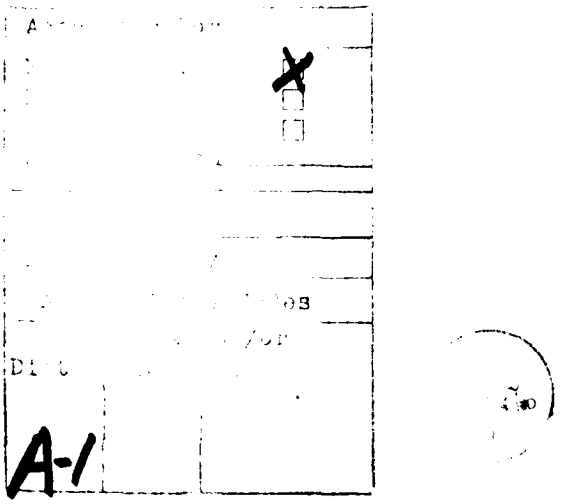

EFFECT OF ENGINE DISCHARGING JET EFFLUX ON VEHICLE AERODYNAMIC PERFORMANCE

by

Dao-wei Yang

ABSTRACT Based on the fundamental theories of gas dynamics, this paper discusses the general effects of the engine discharging jet efflux (EDJE) on the flow around a vehicle (FAV), and analyzes the effect of the high temperature EDJE on vehicle aerodynamic performance, using compressed air in wind-tunnel test to simulate the high temperature EDJE in a real jet engine. Experimental results are cited and analyzed.

NOMENCLATURE

A	= cross-sectional area of the nozzle exit
$C\mu$	= momentum coefficient
$\dot{m}$	= efflux mass flux
m_{z1}	= vehicle pitching moment coefficient in the presence of the jet efflux
m_{z0}	= vehicle pitching moment coeeficient in the absence of the jet efflux
Δm_z	= increment of the vehicle pitching moment coefficient, $\Delta m_z = m_{z1} - m_{z0}$.
p_e^*	= total pressure of the jet efflux at the cross-section of the nozzle exit
q_∞	= freestream dynamic pressure
$q(\lambda_e)$	= flow volume function
S	= vehicle wing area

Received June 11, 1983; revised copy finalized February 25, 1984

V = velocity of fluid

α = vehicle's angle of attack

λ_e = efflux velocity coefficient at the cross-section of the nozzle exit

$\pi(Ma_e)$ = gas dynamic function

ρ_∞ = density of the freestream

φ = yaw angle of the vehicle horizontal tail

SUBSCRIPTS

a = air

b = flow around the body

e = efflux at the cross-section of the nozzle exit

g = combustion gas

∞ = freestream conditions

f = object

m = model

1. INTRODUCTION

The effect of the EDJE of the FAV can be summed up as the streamline displacement effect and the injection effect. When a vehicle flies at supersonic speed, the EDJE effect can only be disseminated through the subsonic region within the boundary layers to the upper reaches. In this case, the EDJE has minute influence on the vehicle dynamic performance, except on the drag force on the lower surface. When the FAV is subsonic, however, this EDJE effect can be disseminated up to the upper reaches, such that it can impair aerodynamic performance of the whole vehicle. It is, therefore, of practical significance to perform such kind of tests.

2. SIMULATION PARAMETERS TESTING

In the wind-tunnel test, we substituted compressed air for the combustion gas to simulate the real conditions where the influence of the EDJE on the FAV was studied. Here, not only the simulation criteria required for a routine

wind-tunnel test should be ensured, but also the characteristics of the influence of the EDJE on the FAV must be simulated, i.e., keeping the FAV streamline shape and wave mode of the model the same as during a real flight. Thus, the pressure drop ratio $(p_e^*/p_b)_m$ or the back pressure ratio $(p_b/p_e^*)_m$ at the nozzle exit of the EDJE of the model engine must be equal to that during a real flight, i.e., $(p_b/p_e^*)_m = (p_b/p_e^*)_f$.

Since
$$\frac{p_b}{p_0^*} = \frac{p_b}{p_e}\ \frac{p_e}{p_0^*} \tag{2.1}$$

then
$$\frac{p_e}{p_0^*} = \pi(Ma_e) = 1\Big/\left(1+\frac{\gamma-1}{2}M_{0e}^2\right)^{\frac{\gamma}{\gamma-1}} \tag{2.2}$$

When neglecting the difference in the combustion gas specific heat to air specific heat ratio between these two conditions, the Mach number at the nozzle exit, Ma_e and the FAV to the jet efflux static pressure ratio p_b/p_e are simulated.

Since
$$\frac{\dot{m}V_e}{A} = \gamma\left(\frac{2}{\gamma+1}\right)^{\frac{\gamma}{\gamma-1}} p_0^*\lambda_e q(\lambda_e) \tag{2.3}$$

then
$$\frac{p_\infty}{p_0^*} = \frac{p_\infty}{p_b}\ \frac{p_b}{p_0^*} \tag{2.4}$$

When the freestream static pressure of the model, p_∞ equals that of the real vehicle, then $\left(\frac{p_\infty}{p_b}\right)_m = \left(\frac{p_\infty}{p_b}\right)_f$, since the flow conditions for the model and the real vehicle are similar to each other.

If $\left(\frac{p_b}{p_0^*}\right)_m = \left(\frac{p_b}{p_0^*}\right)_f$, then $p_{0m}^* = p_{0f}^*$.

From eqn. 2.3, it follows that
$$\left(\frac{\dot{m}V_e}{A}\right)_m = \left(\frac{\dot{m}V_e}{A}\right)_f \tag{2.5}$$

where the momentum flux at the cross-section is also simulated. Since the freestream dynamic pressure is
$$q_\infty = \frac{1}{2}\rho_\infty V_\infty^2 = \frac{1}{2}\gamma p_\infty M_\infty^2 \tag{2.6}$$

from the definition of the momentum coefficient, then
$$C_e = \frac{\dot{m}V_e}{q_\infty S} = \frac{\dot{m}V_e}{Aq_\infty}\ \frac{A}{S} \tag{2.7}$$

It can be shown, from eqns. 2.6 and 2.7, that the same freestream Mach number, Ma_∞ and the same static pressure, p_∞ for the model and for the real vehicle can ensure for the model the same freestream dynamic pressure as that for the real vehicle. Also, from geometric similarity, $\left(\frac{A}{S}\right)_m = \left(\frac{A}{S}\right)_f$. Thus, when simulating the back pressure ratios, an equality of the momentum coefficients

for the model and the real vehicle can be reached.

In summary, when the model is geometrically similar to a real vehicle, and has the same freestream Mach number, the same freestream static pressure and the same pressure drop ratio at the nozzle exit as the real vehicle, they will definitely have the same Mach number at the nozzle exit, the same momentum flux at the cross-section of the nozzle exit and the same jet momentum coefficient. Thus, the flow conditions of the efflux and the FAV in the vicinity of the nozzle exit are similar to those for a real vehicle.

3. RESULTS AND DISCUSSION

The test was conducted using compressed air in a slow speed wind-tunnel to investigate the effect of the EDJE on vehicle dynamic performance. Fig. 3.1 shows the principles of the test. The compressed air used had been dried. The pressure of the air source in this test ranged from 3.43×10^6 to 11.77×10^6 Pa. A control valve lowered the pressure to the required region. Compressed air passed from a ground pipe through a special flexible rubber tubing to the wind-tunnel and the model. It has been shown that this connection does not have any effect on the conduction ratio of the wind-tunnel balance. The vehicle has an engine with a converging jet nozzle. The wings are mounted in the middle of the vehicle and are far from the nozzle, while the horizontal tail is fixed on the rear part of the body and near the nozzle. Results show that the jet efflux has little influence on the lift and drag coefficients but appreciably affects the pitching moment coefficient. The present paper only discusses the effect of the jet efflux on the vehicle pitching moment coefficient, using the increments of the coefficient.

3.1. Effect of the Yaw Angle of the Horizontal Tail

The effect of the yaw angle of the horizontal tail on the increment of the vehicle pitching moment coefficient due to the jet efflux is shown in Fig. 3.2. The curve in the figure was obtained under the following conditions: the freestream dynamic pressure, $q_\infty = 1275.3$ Pa, the efflux pressure drop ratio,

p_e^* / p_∞ = 2.0 and the vehicle angle of attack, α = 0. It is shown in Fig. 3.2 that when φ = 0°, the vehicle obtained a small additional upward moment due t the jet efflux. As the negative yaw angle increases, this additional upward moment increases, reaches the maximum value at the median yaw angles, then decreases. As the positive φ increases, this additional upward moment decreases rapidly and vanishes, then changes to a downward moment. This is due to the injection effect of the jet efflux on the air stream in the vicinity of the model. First of all, the local dynamic pressure at the horizontal tail increases, resulting in another increase in the load of the horizontal tail. At the same time, this injection can also change the pressure profiles in the longitudinal and lateral directions on the upper and lower surfaces of the horizontal tail, that is, when φ is negative, more volume of flow is carried away in unit time at the lower part of the tail than at the upper part, resulting in larger increase in the velocity of the air flow and larger pressure drop at the lower surface than at the upper surface. Therefore, an additional upward moment is obtained due to the jet efflux effect. As the negative yaw angle of the horizontal tail increases, this additional moment increases due to stronger effect on the injection of the air stream at the lower part of the horizontal tail. When this negative yaw angle further increases, however, this injection effect for the horizontal tail can cause separation of flow at the lower surface of the tail. In this case, the pressure drop at that surface decreases as the negative angle of yaw increases, thus decreasing in the increment of the additional upward moment of the body.

On the other hand, when the horizontal tail has a positive angle of yaw, the injection effect of the jet efflux on the flow is larger at the upper part of the tail than at its lower part. The body, therefore, produces an additional downward moment due to the jet efflux. Since the rear part of the model vehicle is not symmetrical up and down, and the flow direction of the jet efflux and the horizontal base line of the body do not overlap, this additional moment does not equal zero, when φ = 0°.

3.2. Ground Effect

The ground effect on the vehicle pitching moment coefficient due to the jet efflux is shown in Fig. 3.3. The curves in the figure were obtained under conditions where q_∞ =1275.3 Pa, the efflux pressure drop ratio p_e^*/p_∞ = 2.0, and $\alpha = 10^\circ$. When the yaw angle of the horizontal tail has a negative value, the increment of the upward moment in the presence of ground is larger than that in the absence of ground, due to the injection effect of the jet efflux. The reason for this is that the presence of ground places restrictions on the system, causing stronger injection effect on the flow, and larger decrease in the pressure drop at the lower surface of the tail with larger increment of the body upward moment.

3.3. Effect of the Efflux Pressure Drop Ratio

The effect of the efflux pressure drop ratio on the increment of the vehicle pitching moment coefficient due to the jet efflux is shown in Fig. 3.4. These data points were obtained when $\alpha = 0^\circ$, $\varphi = 0^\circ$ and q_∞ = 1275.3 Pa in the presence of ground. It is shown in the figure that at first Δm_z increases rapidly as the pressure drop ratio increases, then levels off, and finally decreases slightly near $p_e^*/p_\infty = 2.0$; the Δm_z maximum value appears near the local critical pressure drop ratio at the nozzle exit, i.e., near p_e^*/p_e = 1.893.

Since $\frac{p_e^*}{p_\infty} = \frac{p_e^*}{p_e}\,\frac{p_e}{p_\infty}$, and the presence of the vehicle, $\frac{p_e}{p_\infty} < 1$,

Thus $\frac{p_e^*}{p_e} = 1.893$, when $\frac{p_e^*}{p_\infty} < 1.893$.

Since, in the case of small pressure drop ratios, the velocity of the efflux increases more rapidly as this ratio increases, the injection effect becomes increasingly larger. With large pressure drop ratios, however, change in the injection effect is small, as the ratio changes. When this ratio is larger than its critical value, the efflux continues to expand, then reaches subsonic speed at the nozzle exit. Its boundary has at first diverging then converging shapes, and the streamline of the FAV displaces. It is this displacement that most likely weakens the influence of the efflux on the injection of the FAV, resulting in a decrease in the increment, Δm_z.

3.4. Freestream Effect

The freestream effect on the increment of the vehicle pitching moment coefficient due to the jet efflux is shown in Fig. 3.5. The curve in the figure was drawn based upon the data obtained when $\alpha = 0°$, $\varphi = 0°$ and $p_e^*/p_\infty = 2.0$ in the presence of ground. It is apparent from the figure that the increment decreases as the freestream velocity increases. This is because when the efflux pressure drop ratio is kept constant, the injection effect is reduced as the freestream velocity increases.

3.5. Effect of the Gas Specific Heat Ratio

The simulation test was conducted in a wind-tunnel using compressed air to substitute for the combustion gas. From the formulas relavant to the simulation parameters in the test, it is shown that the difference between the parameters of the compressed air and those of the combustion gas results only from γ, not from the gas constant, R. So, this paper only discusses the γ effect, and gives example calculations for $\frac{p_e^*}{p_c}=2.0, \gamma_a=1.40, \gamma_g=1.33,$ and $\gamma_g=1.20$, assuming $p_c = 1\times10^5 \mathrm{Pa}$.

$$\frac{p_c}{p_e^*}=\left(1-\frac{\gamma-1}{\gamma+1}\gamma_e^2\right)^{\frac{\gamma}{\gamma-1}}$$

From

$$\lambda_e=\sqrt{\frac{\gamma+1}{\gamma-1}\left[1-\left(\frac{p_c}{p_e^*}\right)^{\frac{\gamma-1}{\gamma}}\right]} \tag{3.1}$$

then

$$Ma_e=\sqrt{\frac{\frac{2}{\gamma+1}\lambda_e^2}{1-\frac{\gamma-1}{\gamma+1}\lambda_e^2}} \tag{3.2}$$

$$q(\lambda_e)=\left(\frac{\gamma+1}{2}\right)^{\frac{1}{\gamma-1}}\lambda_e\left(1-\frac{\gamma-1}{\gamma+1}\lambda_e^2\right)^{\frac{1}{\gamma-1}} \tag{3.3}$$

$$\frac{mV_e}{A}=\gamma\left(\frac{2}{\gamma+1}\right)^{\frac{\gamma}{\gamma-1}}p_e^*\lambda_e q(\lambda_e) \tag{3.4}$$

$$\frac{\left(\frac{mV_e}{A}\right)_g}{\left(\frac{mV_e}{A}\right)_a}=\frac{C_{m_g}}{C_{m_a}} \tag{3.5}$$

The following table lists the results of the calculations

γ	λ_e	Ma_e	$\frac{mV_e}{A}$, Pa	$\frac{\lambda_{eg}}{\lambda_{ea}}$	$\frac{Ma_{eg}}{Ma_{ea}}$	$\frac{\left(\frac{mV_e}{A}\right)_g}{\left(\frac{mV_e}{A}\right)_a}$	$\frac{C_{m_g}}{C_{m_a}}$
1.40	1.038	1.046	1.533×10^5	1.0	1.0	1.0	1.0
1.33	1.056	1.066	1.513×10^5	1.017	1.019	0.990	0.990
1.20	1.095	1.107	1.470×10^5	1.055	1.049	0.959	0.959

It is shown from the table that when $p_e^*/p_c = 2.0$ and $\gamma_g = 1.33$, the Mach number of the combustion gas has an 1.9% increase over that of the air, and the momentum flux and momentum coefficient at the cross-section decrease by 1%. When $p_e^*/p_c = 2.0$ and $\gamma_g = 1.20$, the former increases by 4.9% and the latters decrease by 4.1%. Fig. 3.4 reveals that when the pressure drop ratio changes

at $p_e^*/p_\infty \geqslant 1.3$, the increase in the vehicle pitching moment coefficient due to the jet efflux is not appreciable. This simulation test is, therefore, considered feasible using compressed air to substitute for the combustion gas

4. CONCLUSIONS

(1) Based upon the analysis of the effect of the EDJE on the FAV, it is shown that when the FAV is supersonic, the EDJE effect on vehicle aerodynamic performance (except the drag force on the lower surface) is minimal, when the FAV is subsonic, this effect is considerably large. By performing such tests, more accurate aerodynamic data will be provided for the newly-developed vehicles.

(2) When a model is geometrically similar to a real vehicle and has the same freestream Mach number, the same freestream static pressure, and the same pressure drop ratio at the nozzle exit as the vehicle, it can be ensured that its Mach number at the nozzle exit, the momentum flux at the exit cross-section and the efflux momentum coefficient are the same as those for the real vehicle thus the flow conditions of the jet efflux and the FAV in the vicinity of the exit are similar to those of the real one. As shown from the calculations and the experimental results, the gas specific heat ratio has nothing to do with the vehicle aerodynamic performance. It is, therefore, feasible to investigate the effects of the EDJE on vehicle aerodynamic performance in a slow speed wind-tunnel using compressed air to simulate the high temperature combustion gas in a real vehicle.

REFERENCES

1. Northwestern University of Technology, Nanjing Aeronautical Institute and Beijing Aeronautical Institute, Ed., FUNDAMENTALS OF GAS DYNAMICS, Defence Industry Publishing House, Beijing, June, 1980.
2. Maurice J. Zucrow and Joe D. Hoffman, GAS DYNAMICS, John Wiley & Sons, Inc., 1976.
3. R. C. Bankster and D. W. Herter, Chinese Translation by Tai-qian Xu, WIND-

TUNNEL EXPERIMENTAL TECHNIQUES, Defence Industry Publishing House, Beijing February 1964.

4. M. S. Alan Pope, WIND-TUNNEL TESTING, John Wiley & Sons, Inc., 1954.

Figure Caption

Fig. 3.1. The principles of the test.

1- valve; 2- control valve; 3- thermometer; 4- gauge; 5- compressed air

Fig. 3.2. Effect of the yaw angle of the horizontal tail of Δm_z.

Fig. 3.3. Effect of ground on Δm_z.

1- in the presence of ground; 2- in the absence of ground.

Fig. 3.4. Effect of the efflux pressure drop ratio on Δm_z.

Fig. 3.5. Effect of the freestream velocity on Δm_z.

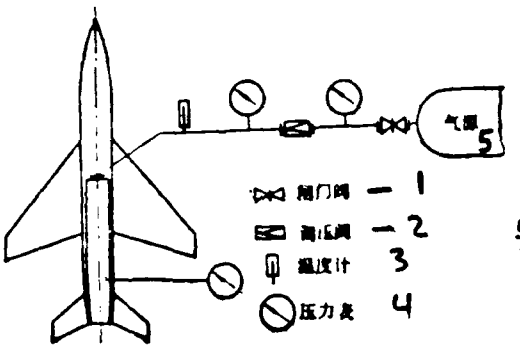

图3.1 试验装置原理图

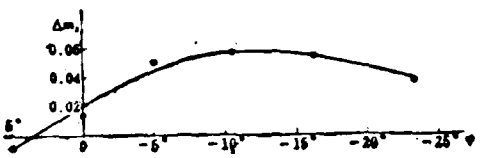

图3.2 平尾偏角φ对Δm_z的影响

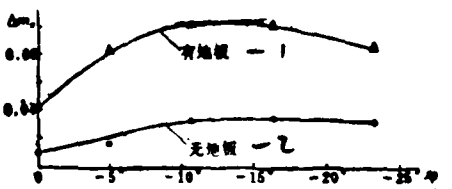

图3.3 地面效应对Δm_z的影响

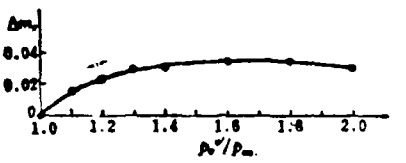

图3.4 喷流落压比对Δm_z的影响

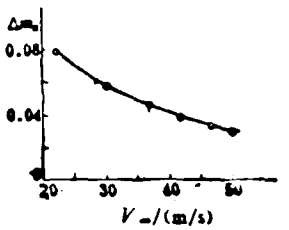

图3.5 来流速度对Δm_z的影响

END

DTIC

5-86